# Thermal performance evaluation of an indirect solar dryer

**Koua Kamenan Blaise[1,2,*], Koffi Ekoun Paul Magloire[1], Gbaha Prosper[1]**

1. *Laboratoire d'Energies nouvelles et Renouvelables, UMRI 58, Institut National Polytechnique Félix Houphouët Boigny, B.P. 581 Yamoussoukro, Cote d'Ivoire*

2. *Laboratoire d'Energie Solaire, UFR SSMT, Université Félix Houphouët Boigny, 22 B.P. 582 Abidjan 22, Cote d'Ivoire*

*kbkoua@yahoo.com*

ABSTRACT. *The thermal performance of an indirect forced convection solar dryer was investigated experimentally with cocoa beans as drying products. The dryer mainly consists of a solar collector, a drying chamber and two fans. Two photovoltaic panels and battery storage are also integrated with the dryer to supply the required electrical energy. Experiments were performed for three different meteorological conditions. The results show a temperature for air inside the solar collector rise of 22.1 °C, 15.6 °C and 13.2 ° C with respect to the ambient air temperature, for the sunny day, partially covered day and cloudy day, respectively. The average solar flux on the collector was 644 W/m2, 448 W/m2 and 341 W/m2, for the sunny day, partially covered day and cloudy day, respectively. The thermal efficiency of the solar collector varied between 34.89 % and 43.40 % whatever the type of day. The thermal drying efficiency of the indirect solar dryer varied between 14.48 % and 20.17 %. The hourly variation of drying chamber temperature is much higher than the ambient air temperature during the experiments.*

RÉSUMÉ. *La performance thermique d'un séchoir solaire indirect à convection forcée d'air a été étudiée expérimentalement avec des fèves de cacao comme produits de séchage. Le séchoir comprend principalement un capteur solaire, une chambre de séchage et deux ventilateurs. Deux panneaux photovoltaïques et une batterie de stockage sont également intégrés au séchoir pour fournir l'énergie électrique requise pour le fonctionnement des ventilateurs. Des expériences ont été effectuées pour trois conditions météorologiques différentes. Les résultats montrent que la température de l'air à l'intérieur du capteur solaire a augmenté de 22,1 °C, 15,6 °C et 13,2 °C par rapport à la température de l'air ambiant, pour le jour ensoleillé, le jour partiellement couvert et le jour nuageux, respectivement. Le flux solaire moyen sur le collecteur était de 644 W/m2, 448 W/m2 et 341 W/m2, respectivement pour le jour ensoleillé, le jour partiellement couvert et le jour nuageux. Le rendement thermique du capteur solaire variait entre 34,89 % et 43,40 % quel que soit le type de jour. Le rendement thermique de séchage du séchoir solaire indirect a varié entre 14,48 % et 20,17 %. La variation horaire de la température de la chambre de séchage est beaucoup plus élevée que la température de l'air ambiant au cours des expériences.*

Instrumentation, Mesure, Métrologie – n° 1/2018, 131-151

*KEYWORDS : indirect solar dryer, thermal efficiency, temperature, solar radiation.*
*MOTS-CLÉS: séchoir solaire indirect, rendement thermique, température, fxlux solaire.*

DOI:10.3166/I2M.17.131-151 

## 1. Introduction

Solar deposit is one of the most important non-polluting and economic sources of energy on an international scale. Solar energy is utilized in many ways including heating, cooling, converting into electricity and many more. Among many of the applications, solar drying is one of the important means of utilizing solar energy for low and moderate temperature applications. The drying process is one of the well-known methods for preservation of the foodstuffs. This process prevents occurrence of unpleasant changes such as microbial spoilage and enzymatic reaction by removing water from food products. Moreover, drying by lowering the mass and volume of food products reduces the cost of packaging, storage and transportation (Goyal *et al*., 2006; Darvishi *et al*., 2016)

Considerable efforts have been made to design and develop solar dryers for drying of agricultural products in developing countries. The solar dryers make use of a closed space which accommodates the product being dried; this gives better and hygienic results. An effective solar dryer is a dryer that allows quick drying without degradation of the products to be dried. This guy of dryers depends on the weather conditions that affect accordingly, the variables inside the dryer (temperature and humidity) that are able to optimize the criteria of appreciation of drying (Souza *et al*., 2015). The knowledge of the climatic characteristics of the region where the solar dryer will be installed is therefore necessary.

Evaluation of a drying system provides relevant information on thermal and drying efficiencies, facilitating improvements in its design (Lopez-Vidana *et al.*, 2013). The principle components of solar dryers are the solar collector and the drying chamber. The solar air collector is considered to be a simple device consisting of one transparent cover situated above an absorbing plate with the air flowing under absorber plate (Chabane *et al*., 2014). The conventional solar air collector has been investigated for heat transfer efficiency improvement by introducing forced convection (Tonui and Tripanagnostopoulos, 2007; Gao *et al*., 2007; Verma and Prasad, 2000). The most determining parameters in thermal efficiency include design, collector manufacturing materials, absorbing plate geometry and coat paint, angle of inclination, and air flow velocity inside the collector. The drying efficiency makes it possible to evaluate the effects of other parameters that intervene in the process, such as drying rate, air flow distribution, and temperature inside the drying chamber (Singh and Kumar, 2012). Since operating conditions and food characteristics have significant influence on drying efficiency, even a given dryer tested with same food product for different operating conditions or different food products with same operating condition may not give consistent efficiency results (Singh and Kumar, 2012). This paper aims to study the thermal behaviour of each unit of the indirect solar dryer under the different climate conditions.

## 2. Materials and methods

### *2.1. Description of the indirect solar dryer*

As shown in Fig. 1, the indirect solar dryer consists mainly of a solar air collector system and a drying chamber containing tree rectangular trays and a flux diffuser. The flux diffuser is a performed surface through which the hot air arriving from the solar collector passes and exiting through the holes creates a uniformly distributed flow. The solar air collector system was used to produce thermal energy for drying. The solar air collector consists of glass cover and aluminium absorber plate which is painted with black paint in order to increase the absorption for the global solar radiation beam and diffuse light. It is tilted to an angle of 7° with respect to horizontal surface. The solar air collector has a useful collector area of 2 $m^2$, and a channel size of 2.5 cm high. The edge and bottom surfaces are thermally insulated with a 5 cm thick polystyrene layer.

Two fans that are driving by photovoltaic panels regulate the airflow. A battery storage in integrated with the photovoltaic panels and it supplies the required energy when solar energy is not available. This allows the autonomous operation of the indirect solar dryer.

*Figure 1. Picture of the indirect solar dryer*

### *2.2. Experimental procedure*

Fermented cocoa beans were spread thinly in one bean layer on tree trays inside the drying chamber. Drying was terminated when the cocoa bean weight became constant between two measurements. The moisture content of cocoa beans at any time of drying (X) was determined from mass measurements as:

$$X = \frac{m_t - m_d}{m_d} \quad (1)$$

where $m_d$ and $m_t$ is the dry mass and the mass at any drying time of cocoa bean, respectively.

During the drying process, the total incident solar radiation was measured using a pyranometer Kipp and Zonen CM 10. Type K thermocouples constituted by the couple of conductor (Nickel 10% Chrome (+)/Nickel 5% Aluminum (-)) were used for measurement of the temperatures inside the indirect solar dryer. The data acquisition was carried out manually using a Voltcraft PL-120-T2 digital thermometer.

### *2.3. Drying kinetic*

The kinetics of drying results from two factors of resistance to drying: the exchange of vapour at the product-air interface and the resistance to the transport of the fluid within the solid matrix. In order to take into account the effect of volume shrinkage, the mass flux ($F_m$) at different instants of drying was estimated according to Eq. (2) (Dissa *et al*., 2010).

$$F_m = -\left(\frac{\rho_d}{\beta}\right)\frac{dX}{dt} = -\left(\frac{m_d}{A}\right)\frac{dX}{dt} \quad (2)$$

where $\rho_d$ is the bulk density of dry product, A is the exchange surface of the product and β is the compactness.

The drying rates (dX/dt) were calculated by approximation of the derivatives to finite differences based on the following Eqs. (3) – (5):

$$\frac{dX}{dt} = \left(\frac{X_1 - X_0}{t_1 - t_0}\right) \text{ at initial instant } t_0 \quad (3)$$

$$\frac{dX}{dt} = \left(\frac{X_n - X_{n-1}}{t_n - t_{n-1}}\right) \text{ at instant } t_n \text{ of the end of drying} \quad (4)$$

$$\frac{dX}{dt} = \frac{1}{2}\left(\frac{X_i - X_{i-1}}{t_i - t_{i-1}} + \frac{X_{i+1} - X_i}{t_{i+1} - t_i}\right) \text{ at each instant } t_i \text{ for i between 1 and } n-1 \quad (5)$$

### *2.4. Thermal performance analysis*

The system studied is an indirect solar dryer operating in forced convection, which, by an autonomous operation mode, leads to a good efficiency as well as to a good quality of the dried product. It is a system without storage or recycling of air.

#### *2.4.1. Solar collector*

The thermal performance of the solar collector is analyzed in transitory state throughout a day of experience. The uncontrollable and unpredictable nature of the parameters involved in solar drying systems is an obstacle to exact theoretical study (Lopez-Vidana *et al.*, 2013; Karim and Hawlader, 2008). In transitory state operating conditions, an evaluation of solar collector performance is the instantaneous thermal efficiency of the solar collector, η, which is defined as ratio of useful energy gain, $q_u$, over a specific time period to the incident solar energy over the same period.

$$\eta = \frac{\int_0^t q_u dt}{A_c \int_0^t I_t dt} \tag{6}$$

The factor $I_t$ is the incident solar irradiation and Ac is the solar collector area.

The useful heat gain of a solar collector, $q_u$, can be expressed as (Koyuncu, 2006; Singh and Dhiman, 2016):

$$q_u = \dot{m} C_{pa} (T_0 - T_i) \tag{7}$$

In stationary state, the thermal performance of a solar collector can be expressed by the Hottel-Whillier et Bliss equation (Singh and Dhiman, 2016; Karim and Hawlader, 2004):

$$q_u = A_c F_R \left[ (\tau\alpha)_n - U_L (T_i - T_{am}) \right] \tag{8}$$

The thermal efficiency of the solar collector can therefore be expressed as:

$$\eta = \frac{q_u}{A_c I_t} = \dot{m} C_{pa} \frac{(T_0 - T_i)}{A_c I_t} = F_R \left[ (\tau\alpha)_n - U_L \frac{(T_i - T_{am})}{I_t} \right] \tag{9}$$

Where $T_0$ and $T_i$ are the air temperatures at the outlet and inlet of solar collector, respectively; $T_{am}$ is the ambient temperature; $C_{pa}$ is the air specific heat and $\dot{m}$ is the air mass flow. *FR* is the solar collector heat removal factor. It is expressed as (Singh and Dhiman, 2016; Nematollahi *et al.*, 2014):

$$F_R = \frac{\dot{m} C_{pa}}{U_L}\left[1 - \exp\left(-\frac{F' U_L}{\dot{m} C_{pa}}\right)\right] \quad (10)$$

where F' is the solar collector efficiency factor defined as the ratio of the actual useful gain to the useful energy gain that would result if the solar collector absorbing surface were at the local fluid temperature. This factor is essentially a constant for any given solar collector design and fluid flow rate (Singh and Dhiman, 2016).

$U_L$ is the overall thermal loss coefficient of the solar collector. It is equal to the sum of energy loss through the top, bottom and sides of the solar collector (Lopez-Vidana *et al*., 2013; Koyuncu, 2006).

Plot between instantaneous efficiency of the solar collector and temperature rise parameters $(T_i - T_{am})/I_t$ is represented by straight line if overall loss coefficient $U_L$, heat removal factor $F_R$ and transmittance absorptance product $(\tau\alpha)_n$ are constants. The y-intercept and the slope of the straight line (represented by Eq. (8)) yields the values of $F_R(\tau\alpha)_n$ and $F_R U_L$, respectively.

Product absorptance-transmittance $(\tau\alpha)_n$ was determined through optical analysis of the system of the transparence cover, using Eq. (11) (Lopez-Vidana *et al*., 2013; Kalogirou, 2009):

$$(\tau\alpha)_n = 0{,}96(\tau\alpha) \quad (11)$$

where $(\tau\alpha)$ is the effective radiation.

From the Eq. (9), the variation of the air temperature between the outlet and the inlet of the solar collector can be written in the form:

$$T_0 - T_i = \frac{A_c F_R}{\dot{m} C_{pa}}\left[(\tau\alpha)_n I_t - U_L (T_i - T_{am})\right] \quad (12)$$

The Eq. (12) can be put into the form:

$$T_0 - T_i = \frac{A_c F_R (\tau\alpha)_n}{\dot{m} C_{pa}} (I_t - I_{tmin}) \quad (13)$$

where

$$I_{tmin} = U_L \frac{T_i - T_{am}}{(\tau\alpha)_n}$$

$I_{tmin}$ is the threshold level of the solar incident radiation (Karim and Hawlader, 2004). If the inlet air temperature is close to that of ambient air, then the $(T_0 - T_i)$ versus $I_t$ points lie on a straight line.

*2.4.2. Drying chamber*

In thermodynamic, thermal efficiency is one of the performance criteria of a device that uses thermal energy. This thermal efficiency indicates the efficacy of a process of conversion or transfer of energy. In terms of drying, the thermal efficiency is defined as the ratio between the latent heat of vaporization of the water of the product and the quantity of energy required to evaporate this water (Torki-Harchegani *et al*., 2016).

Since the indirect solar dryer operates in forced convection, the thermal drying efficiency is given by the following expression (Augustus Leon *et al.*, 2002):

$$\eta_{s\text{閏}h} = \frac{M(t=0)(X_0 - X_f)L_v}{(X_0 + 1)(A_c I_t + P_{ven})t} \quad (14)$$

where $P_{ven}$ is the electrical power consumed by the two fans; M (t=0) is the initial mass of the fresh cocoa beans and $L_v$ is the latent heat of water vaporization.

## 3. Results and discussion

Experiments on the indirect solar drying of cocoa beans were carried out on the site of our laboratory located at Felix Houphouët Boigny National Polytechnic Institute of Yamoussoukro. The experiments were carried out over several periods and three different meteorological conditions were chosen for the thermal performance study of the indirect solar dryer. It's about:

- Sunny day (clear sky) with an overall daily irradiation of 6073.1 Wh/m$^2$;

- Partially covered day: sunny with many passages of clouds. The daily total irradiation for this day is 4134 Wh/m$^2$;

- Cloudy day: little brightness with a few rifts in the afternoon. The daily total irradiation for this day is 2477 Wh/m$^2$.

### *3.1. Drying kinetic of cocoa beans*

It can be seen from Fig. 2 that the mass flux decreased continuously throughout the drying time. During the drying of the cocoa beans, the resistance to the internal transport of the solid matrix increases and gradually becomes dominant. Mass flux decreases and moisture content of cocoa beans approaches equilibrium moisture content. This indicated that cocoa beans drying process took place in the falling rate period. The basic reason for this decreasing is the high evaporation at the surface due to considerable diffusion rate of the internal water towards the surface (Duc *et al*., 2011). Comparable results have also been reported for various other agricultural products (Hii *et al*., 2009; Liu *et al*., 2012). The mass flux versus drying time is adequately represented by the following relation with $r^2 = 0.998$:

$$F_m = 0.317\ (X_0 - X_{eq})\exp(-0.23t) \quad (15)$$

where $F_m$ is in kg/m$^2$h and t is in hour (h).

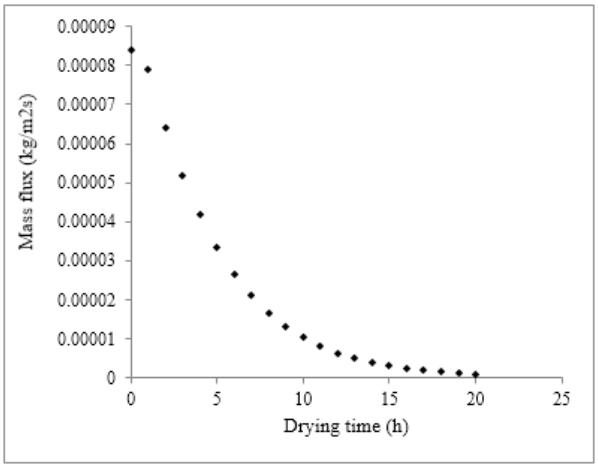


*Figure 2. Variation in mass flux of cocoa beans during indirect solar drying*

### *3.2. Meteorological parameters*

Figure 3a shows that for the sunny day, ambient temperature ($T_{am}$) and solar fluxes (direct, diffuse and global) increase gradually to reach a maximum value before decreasing. The recorded maximum ambient temperature is 39.1 °C at 12 h 20 min. Maximum global solar flux, maximum direct solar flux and maximum diffuse solar flux are of 1075 W/m$^2$, 881.5 W/m$^2$ and 193.5 W/m$^2$, respectively.

Figure 3b shows that for the partially covered day, ambient temperature ($T_{am}$) and solar fluxes (direct, diffuse and global) evolve irregularly. However, the ambient temperature and the different solar fluxes reach their peak at the same time of day, that is at 14 h. The recorded maximum ambient temperature is 37.6 °C. Maximum global solar flux, maximum direct solar flux and maximum diffuse solar flux are of 925 W/m$^2$, 758.5 W/m$^2$ and 166.5 W/m$^2$, respectively.

Figure 3c shows that for the cloudy day, the ambient temperature ($T_{am}$) and the different solar fluxes evolve irregularly. The recorded maximum ambient temperature is 35.5 °C at 13 h. Two solar flux peaks were recorded for the different solar fluxes. The first peak at 13 h with 1093 W/m$^2$, 896.26 W/m$^2$ and 196.74 W/m$^2$ for the global solar flux, the direct solar flux and the diffuse solar flux, respectively. The second peak at 14 h with 1040 W/m$^2$, 852.8 W/m$^2$ and 187.2 W/m$^2$ for global solar flux, direct solar flux and diffuse solar flux, respectively. The recorded ambient temperature at 14 h is 34.6 °C.

In general, the ambient temperature and the different fluxes fluctuate in the same direction. They reach their maximum and minimum value at the same time of day.

The average solar flux on the collector was 644 W/m$^2$, 448 W/m$^2$ and 341 W/m$^2$, for the sunny day, partially covered day and cloudy day, respectively. As far as, the average ambient air temperature was 33.1°C for the sunny day and partially covered day and 30.3 °C for the cloudy day.

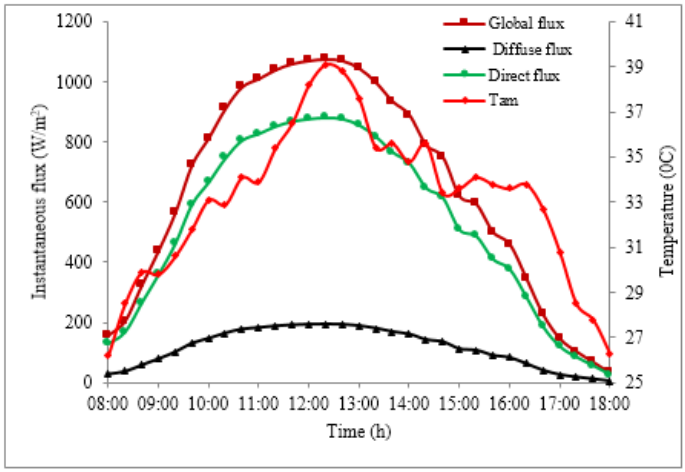


*Figure 3a. Variation of the ambient temperature and the components of the solar flux as a function of time for the sunny day*

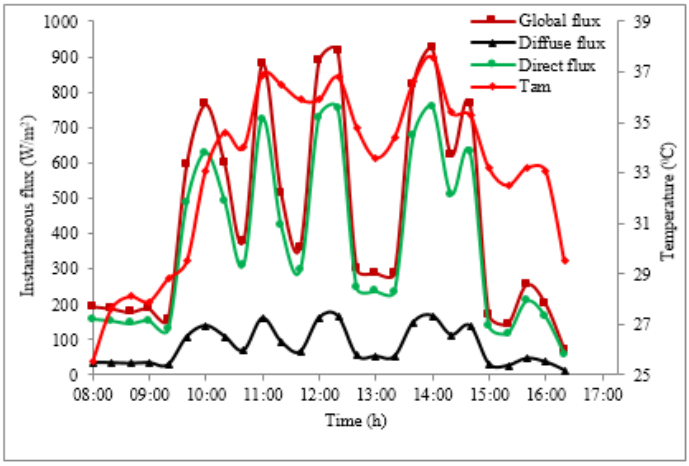


*Figure 3b. Variation of the ambient temperature and the components of the solar flux as a function of time for the partially covered day*

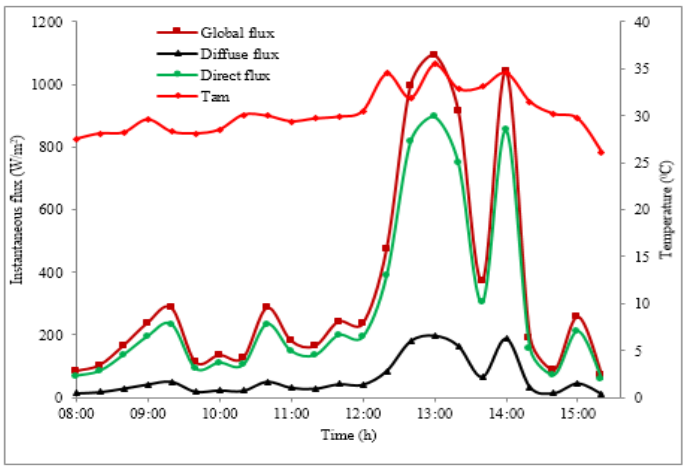


*Figure 3c. Variation of the ambient temperature and the components of the solar flux as a function of time for the cloudy day*

### *3.3. Evolution of temperatures*

Figure 4a shows that for the sunny day, the temperature of the air inside the solar collector ($T_a$), the temperature of the transparent cover ($T_c$) and that of the absorber ($T_{abs}$) evolve increase to reach a maximum value at 12 h 20 min before decreasing. The maximum values recorded for the air temperature inside the solar collector, the temperature of the transparent cover and that of the absorber are 69.8 °C, 63.7 °C and 79.6 °C, respectively. These temperatures are considerably higher than the ambient temperature. The difference temperature between the temperature of the air inside the solar collector and the ambient temperature reaches 30 °C at certain times of the day.

Figure 4b shows that, for the partially covered day, the temperature of the air inside the solar collector ($T_a$), the temperature of the transparent cover ($T_c$) and that of the absorber ($T_{abs}$) evolve irregularly. However, they reach their maximum value at 14 h. The maximum temperature of the air inside the solar collector, the maximum temperature of the transparent cover and that of the absorber are 66.8 °C, 44.3 °C and 68.5 °C, respectively. All these temperatures are therefore considerably higher than the ambient temperature. The difference temperature between the temperature of the air inside the solar collector and the ambient temperature reaches 29 °C at certain times of the day.

Figure 4c shows that, for the cloudy day, the temperature of the air inside the solar collector ($T_a$), the temperature of the transparent cover ($T_c$) and that of the absorber ($T_{abs}$) evolve irregularly. However, all these temperatures are significantly higher than the ambient temperature. Two temperature peaks are recorded at 13h and 14 h, respectively. The difference temperature between the temperature of the air inside the solar collector and the ambient temperature reaches 23 °C at certain times of the day.

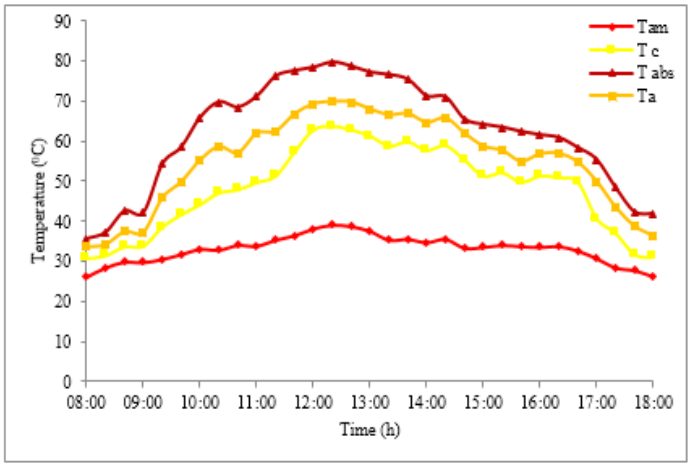


*Figure 4a. variation of the ambient temperature, the temperature of the air inside the solar collector, the temperature of the transparent cover and that of the absorber as a function of time for the sunny day*

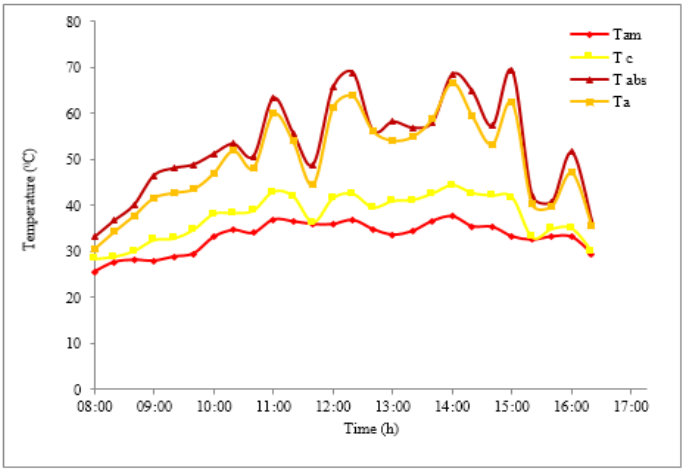


*Figure 4b. variation of the ambient temperature, the temperature of the air inside the solar collector, the temperature of the transparent cover and that of the absorber as a function of time for the partially covered day*

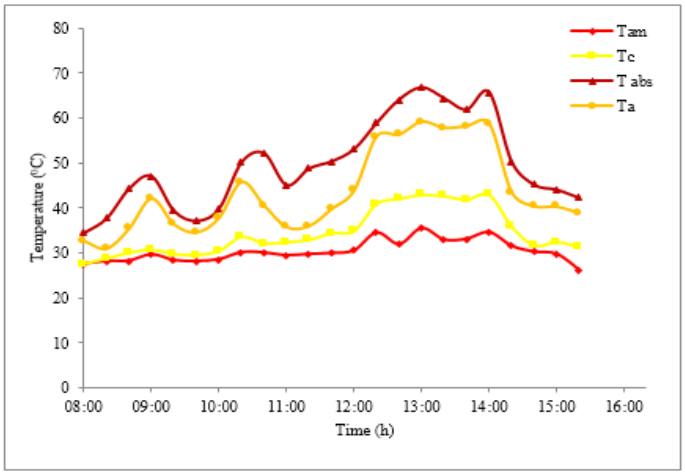


*Figure 4c. variation of the ambient temperature, the temperature of the air inside the solar collector, the temperature of the transparent cover and that of the absorber as a function of time for the cloudy day*

The average air temperature inside the solar collector was 55.2 °C, 49.7 °C and 43.5 °C for the sunny day, partially covered day and cloudy day, respectively. As it is clear, whatever the type of day, the increase of the solar flux leads to an increase of these different temperatures. During the early hours of the morning, the different temperatures are very low due to low solar radiation reaching the earth. However, the temperature of the absorber is always higher than that of the other components. These results have been reported by other authors (Nematollahi *et al*., 2014; Janjai *et al*., 2008; Lee *et al*., 2015).

Figure 5a shows that for the sunny day the temperature of the air at the outlet of the solar collector (Toutput) and that of the air inside the drying chamber (Tinside) increase to reach their maximum value at 12 h 20 min before decreasing. The maximum air temperature at the outlet of the solar collector and the maximum air temperature inside the drying chamber are 66.5 °C and 60.3 °C, respectively. The temperature difference between the temperature of the air inside the drying chamber and the ambient temperature can reach 21 °C at certain times of the day.

Figure 5b shows that for the partially covered day, the temperature of the air at the outlet of the solar collector ($T_{output}$) and that of the air inside the drying chamber ($T_{inside}$) change irregularly. The maximum air temperature at the outlet of the solar collector and the maximum air temperature inside the drying chamber, reached at 14 h, are 56.4 °C. and 43.8 °C., respectively. The temperature difference between the temperature of the air inside the drying chamber and the ambient temperature can reach 10 °C at certain times of the day.

Figure 5c shows that for the cloudy day, the temperature of the air at the outlet of

the solar collector ($T_{output}$) and that of the air inside the drying chamber ($T_{inside}$) evolve irregularly. The maximum air temperature at the outlet of the solar collector and the maximum air temperature inside the drying chamber, reached at 13 h, are 54.6 °C and 43.6 °C, respectively. The temperature difference between the temperature of the air inside the drying chamber and the ambient temperature can reach 8 °C at certain times of the day.

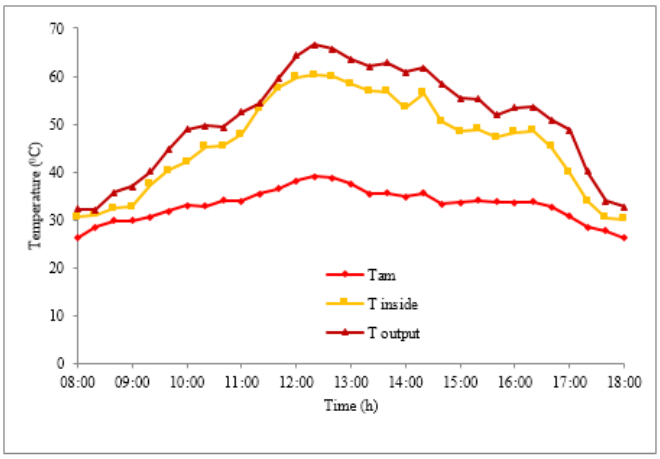


*Figure 5a. Variation of the ambient temperature, the temperature of the air at the outlet of the solar collector and that of the air inside the drying chamber as a function of time for the sunny day*

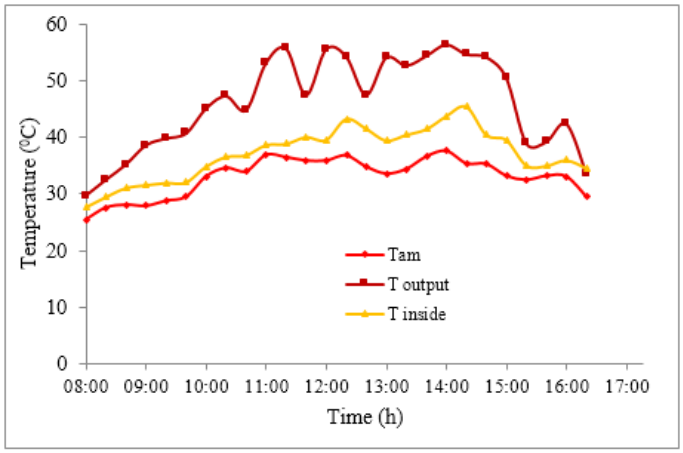


*Figure 5b. Variation of the ambient temperature, the temperature of the air at the outlet of the solar collector and that of the air inside the drying chamber as a function of time for the partially covered day*

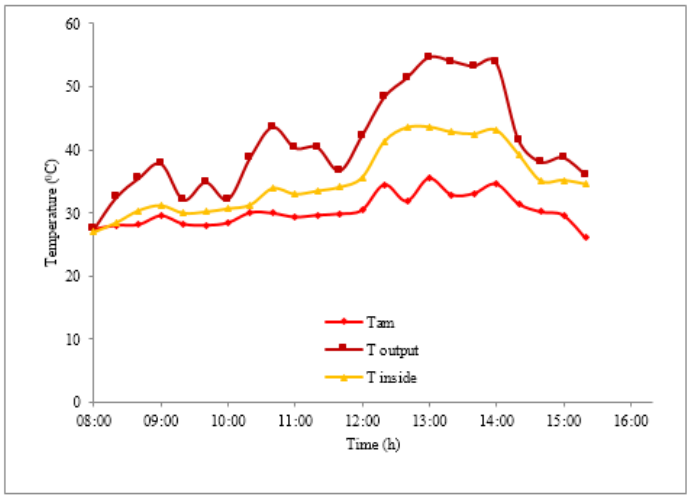


*Figure 5c. Variation of the ambient temperature, the temperature of the air at the outlet of the solar collector and that of the air inside the drying chamber as a function of time for the cloudy day*

The higher the incident solar flux, the higher the air temperature at the outlet of the solar collector (Janjai *et al*., 2008). Increasing the air temperature at the outlet of the solar collector results in an increase in the air temperature inside the drying chamber as shown in Figures 5a, 5b and 5c. Skaar (1988) mentioned that increasing the air temperature by 1°C in a closed drying chamber can reduce the relative humidity of the air by up to 3%. The air inside the drying chamber therefore has a higher absorption power than that of the ambient air, taking into account the temperature of the air inside the drying chamber . The Absorption capacity of the air is a factor in accelerating the evaporation of water from the product to be dried (Joly and More-Chevalier, 1980).

### *3.4. Temperature equation*

Figures 6a, 6b and 6c show the evolution of the air temperature difference between the outlet and the inlet of the solar collector as a function of the incident solar flux, for the sunny day, the partially cloudy day and the cloudy day, respectively. As shown in these Figures, the air temperature difference ($T_0$ - $T_i$) increases linearly as the incident solar flux increases. The comparison between Eq. (12) and the right equations obtained allow to determine the threshold level of the incident solar flux for each type of day (Table 1).

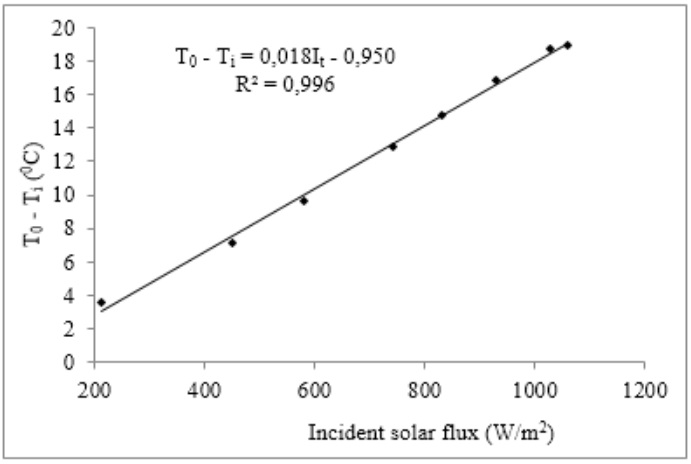


*Figure 6a. Variation of the temperature difference of the air between the outlet and the inlet of the solar collector as a function of the incident solar flux for the sunny day*

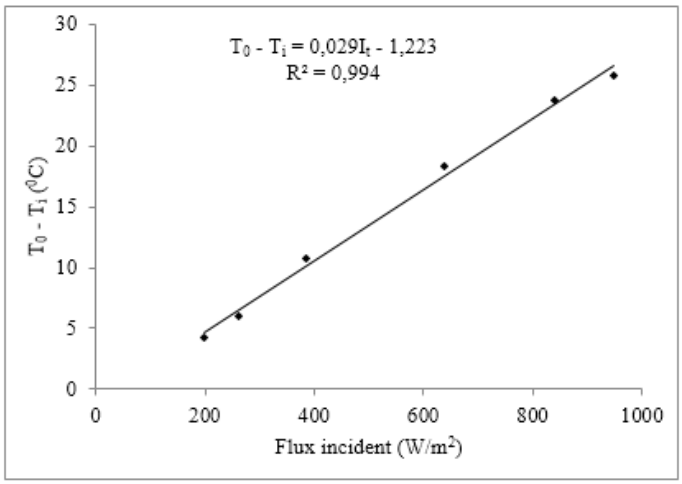


*Figure 6b. Variation of the temperature difference of the air between the outlet and the inlet of the solar collector as a function of the incident solar flux for the partially covered day*

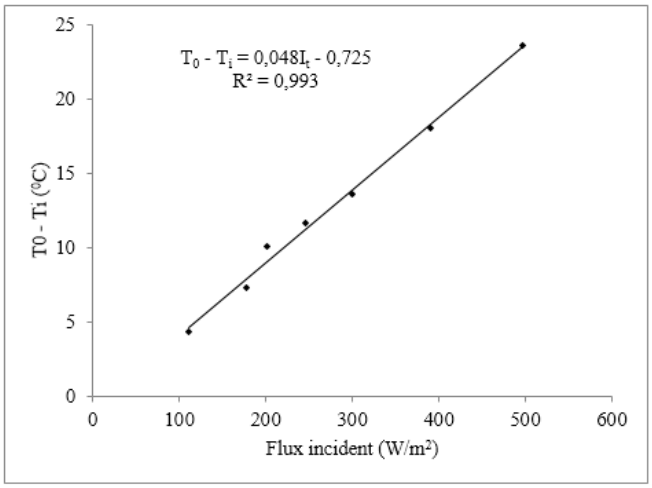


*Figure 6c. Variation of the temperature difference of the air between the outlet and the inlet of the solar collector as a function of the incident solar flux for the cloudy day*

Table 1 shows that the threshold level of the incident solar flux decreases when the intensity of the solar flux decreases. If weather data (temperature, solar flux) are available, these temperature equations are useful for estimating the air temperature at the outlet of solar collector, which is important for the design of a solar dryer for a particular application (Karim and Hawlader, 2004).

It should be noted that the ambient temperature is equal to the air temperature at the inlet of the solar collector (Koyuncu, 2006) and that the mean mass flow of air in the indirect solar dryer is 0.024 kg/s during the experiences.

*Table 1. Temperature equation and threshold level of incident solar flux*

| Type of day | Temperature equation | $\frac{A_c F_R (\tau\alpha)_n}{\dot{m} C_{pa}}$ | $\frac{A_c F_R (\tau\alpha)_n I_{tmin}}{\dot{m} C_{pa}}$ | $I_{tmin}$ | $r^2$ |
|---|---|---|---|---|---|
| Sunny day | $T_0 - T_i = 0.018 I_t - 0.950$ | 0.018 | 0.950 | 52.78 | 0.996 |
| Partially covered day | $T_0 - T_i = 0.029 I_t - 1.223$ | 0.029 | 1.223 | 42.17 | 0.994 |
| Cloudy day | $T_0 - T_i = 0.048 I_t - 0.725$ | 0.048 | 0.725 | 15.10 | 0.993 |

### *3.5. Thermal efficiency of solar collector*

Figure 7 shows the evolution of the thermal efficiency of the solar collector as a function of $(I_i-I_{am})/I_t$ for the three types of day. As can be seen in Fg. 7, the thermal efficiency of the solar collector decreases linearly as the ratio $(I_i-I_{am})/I_t$ increases. The thermal efficiency of the solar collector is higher at the beginning of the day due to the fact that there is little difference between the temperature of the air inside the solar collector and the ambient temperature (Lopez-Vidana *et al*., 2013). Consequently, the radiative and convective losses are also lower. The thermal efficiency of the solar collector is therefore affected by the difference in these temperatures. This difference in temperature is greater at midday and it would therefore be necessary to have a higher air mass flow rate to eliminate excess heat and increase the thermal efficiency by limiting the radiative and convective losses (Lopez-Vidana *et al*., 2013). The average thermal efficiency of the solar collector is 43.40%, 40.84% and 34.89% for the sunny day, the partially covered day and the cloudy day, respectively. It can be said that the thermal efficiency of solar collector increases with increasing solar intensity and mass flow rate as a function of time (Chabane *et al*., 2013). Kumar (2010) found that for solar radiation levels ranging from 550 W/m$^2$ to 850 W/m$^2$, the efficiency varies between 35 % to 40 % for a single pass collector.

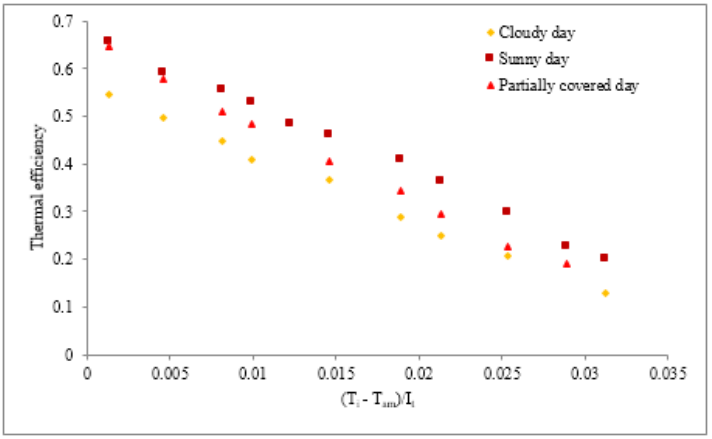


*Figure 7. Variation of the thermal efficiency of the solar collector as a function of $(I_i-I_{am})/I_t$ for the three types of day*

The thermal performance of the solar collector of indirect solar dryer designed in this study shown a fair improvement on state of art and a good agreement exists between the present study and reported systems. Indeed, Koyuncu (2006) obtained a thermal efficiency of 39.05% for a corrugated sheet solar collector. Lopez-Vidana *et al*. (2013) obtained a thermal efficiency of 36% with an air mass flow of 0.434 kg/s for a solar collector with an absorber made of corrugated aluminum sheet.

The linear fit of the three thermal efficiency curves has allowed to obtain the efficient equations given in Table 2. As shown in this Table 2, the overall coefficient of thermal losses $U_L$ of the solar collector is smaller with a greater conductance factor $F_R$ of the absorber for the sunny day. It is also noted that the overall heat loss coefficient and the performance coefficient increase as the temperature difference ($T_i - T_{am}$) increases, leading to decrease in the collector efficiency.

*Table 2. Efficiency equation and physical characteristics of the solar collector*

| Type of day | Efficiency equation | $F_R(\tau\alpha)_n$ | $F_RU_L$ | $F_R$ | $U_L$ | $r^2$ |
|---|---|---|---|---|---|---|
| Sunny day | $\eta$=0.675-15.028*(($T_i$-$T_{am}$)/ $T_t$) | 0.675 | 15.028 | 0.868 | 17.31 | 0.996 |
| Partially covered day | $\eta$=0.654-16.626*(($T_i$-$T_{am}$)/ $T_t$) | 0.654 | 16.626 | 0.841 | 19.77 | 0.996 |
| Cloudy day | $\eta$=0.560-14.032*(($T_i$-$T_{am}$)/ $T_t$) | 0.560 | 14.032 | 0.720 | 19.49 | 0.997 |

### *3.6. Thermal efficiency of drying of the drying chamber*

The thermal efficiency of drying of the indirect solar dryer designed, calculated from Eq. (14) is recorded in Table 3.

*Table 3. Incident solar flux and thermal efficiency of drying*

| | Sunny day | Partially covered day | Cloudy day |
|---|---|---|---|
| Average incident solar flux (W/m$^2$) | 662.16 | 458.63 | 360.29 |
| Thermal efficiency of drying (%) | 18.21 | 20.17 | 14.48 |

The drying efficiency values obtained for the different types of day are within the range of drying efficiency values reported in many literatures on drying. Indeed, Lopez-Vidana *et al*. (2013) obtained a thermal drying efficiency of 15% when their hybrid dryer works only with solar energy. Mechlouch *et al*. (2006) obtained a thermal drying efficiency of 22.5% during the study on the improvement of the thermal efficiency of drying of an indirect solar dryer with an optimal load of 14 kg. As reported by Mohanraj and Chandrasekar (2009) and Misha *et al*. (2015), the thermal efficiency of drying a solar dryer is generally about 20%.

## 4. Conclusion

An indirect type forced convection solar dryer has been designed and fabricated for drying of cocoa beans. A detailed experimental study is conducted to evaluate the thermal performance of the indirect solar dryer under a wide range of operating

conditions. During the drying experiments, the average mass flow rate of the air is 0.024 kg/s. The following conclusions are drawn from the experimental study done in solar dryer:

The hourly variation of drying chamber temperature is much higher than the ambient temperature during the most part of the experimental period;

The solar collector has an average thermal efficiency between 34.89% and 43.40% whatever the type of day. The efficiency of the solar air collectors depends significantly on the solar radiation, mass flow rate, and surface geometry of the collectors.

The thermal drying efficiency of the indirect solar dryer designed varies between 14.48 % and 20.17 %.

The indirect solar dryer designed can be used for drying various agricultural products. It can reduce drying time and improve quality of the dried product.

## References

Augustus Leon M., Kumar S., Bhattacharya S.C. (2002). A comprehensive procedure for performance evaluation of food dryers. *Renewable and Sustainable Energy Reviews*, Vol. 6, pp. 367-393. https://doi.org/10.1016/s1364-0321(02)00005-9

Chabane F., Moummi N., Benramache S. (2013). Experimental analysis on thermal performance of a solar air collector with longitudinal fins in a region of Biskra, Algeria. *Journal of Power Technologies*, Vol. 93, No.1, pp. 52-58.

Chabane F., Moummi N., Benramache S. (2014). Experimental study of heat transfer and thermal performance with longitudinal fins of solar air heater. *Journal of Advanced Research*, Vol. 5, pp. 183-192. https://doi.org/10.1016/j.jare.2013.03.001

Darvishi H., Zarein M., Farhudi Z. (2016). Energetic and exergetic performance analysis and modeling of drying kinetics of kiwi slices. *Journal of Food Science and Technology*, Vol. 53, No. 5, pp. 2317–2333. https://doi.org/10.1007/s13197-016-2199-7

Dissa A. O., Desmorieux H., Savadogo P. W., Segda B. G., Koulidiati J. (2010). Shrinkage, porosity and density during convective drying of spirulina. *Journal of Food Engineering*, Vol. 97, pp. 410-418. https://doi.org/10.1016/j.jfoodeng.2009.10.036

Duc I. A., Han J. W., Keum D. H. (2011). Thin layer drying characteristics of rapeseed (Brassica napus L.). *Journal of Stored Product Research*, Vol.47, pp. 32-38. https://doi.org/10.1016/j.jspr.2010.05.006

Gao W., Lin W., Liu T., Xia C. (2007). Analytical and experimental studies on the thermal performance of cross-corrugated and flat plate solar air heaters. *Applied Energy*, Vol. 84, No.4, pp. 425-441. https://doi.org/10.1016/j.apenergy.2006.02.005

Goyal R. K., Kingsly A., Ramarathinam M., Ilyas S. M. (2006). Thin layer drying kinetics of raw mango slices. *Biosystems Engineering*, Vol. 95, pp. 43-49. https://doi.org/10.1016/j.biosystemseng.2006.05.001

Hii C. L., Law C. L., Cloke M. (2009). Modeling using a new thin layer drying model and product quality of cocoa. *Journal of Food Engineering*, Vol. 90, pp. 191-198. https://doi.org/10.1016/j.jfoodeng.2008.06.022

Janjai S., Srisittipokakun N., Balla B. K. (2008). Experimental and modeling performances of a roof-integrated solar drying system for drying herbs and spices. *Energy*, Vol. 33, pp. 91-103. https://doi.org/10.1016/j.energy.2007.08.009

Joly P., More-Chevalier F. (1980). Théorie, pratique et économie de séchage des bois. Editions H. Vial.

Kalogirou S. (2009). Solar energy engineering: Processes and systems. 1st ed. Elsevier's Science and Technology, Oxford, UK.

Karim M. A., Hawlader M. N. A. (2004). Development of solar air collectors for drying applications. *Energy Conversion and Management*, Vol. 45, pp. 329-344. https://doi.org/10.1016/S0196-8904(03)00158-4

Karim M. A., Hawlader M. N. A. (2008). Performance evaluation of a V-groove solar air collector for drying applications. *Applied Thermal Engineering*, Vol. 26, pp. 121-130. https://doi.org/10.1016/j.applthermaleng.2005.03.017

Koyuncu T. (2006). Performance of various designs of solar air heaters for crop drying applications. *Renewable Energy*, Vol. 31, pp. 1073-1088. https://doi.org/10.1016/j.renene.2005.05.017

Kumar R. (2010). Performance of a double pass solar air collector. *Solar Energy*, Vol. 84, No.11, pp. 1929-1937. https://doi.org/10.1016/j.solener.2010.07.007

Lee D. S., Hung T. C., Lin J. R., Zhao J. (2015). Experimental investigations on solar chimney for optimal heat collector to be utilized in organic Rankine cycle. *Applied Energy*, Vol. 154, pp. 651-662. https://doi.org/10.1016/j.apenergy.2015.05.079

Liu G. H., Chen J. R., Liu M. H., Wan X. (2012). Shrinkage, porosity and density behavior during convective drying of bio-porous material. *Procedia Engineering*, Vol. 31, pp. 634-640. https://doi.org/10.1016/j.proeng.2012.01.1078

Lopez-Vidana E. C., Mendez-Lagrinas L. L., Rodriguez-Ramirez J. (2013). Efficiency of a hybrid solar-gas dryer. *Solar Energy*, Vol. 93, pp. 23-31. https://doi.org/10.1016/j.solener.2013.01.027

Mechlouch R. F., Daoud H. B., Bagane M., Slama R. B., Bouabdellah M. (2006). Amélioration du rendement d'un séchoir solaire indirect. Séminaire Maghrebien sur les sciences et les Technologies de séchage, 17-19 décembre 2006, Tozeur, Tunisie.

Misha S., Mat S., Ruslan M. H., Salleh E., Sopian K. (2015). Performance of a solar assisted solid desiccant dryer for kenaf core fiber drying under low solar radiation. *Solar Energy*, Vol. 112, pp. 194-204. https://doi.org/10.1016/j.solener.2014.11.029

Mohanraj M., Chandrasekar P. (2009). Performance of a forced convection solar drier integrated with gravel as heat storage for chili drying. *Journal of Engineering Science and Technology*, Vol. 4, No. 3, pp. 305-314.

Nematollahi O., Alamdari P., Assari M. R. (2014). Experimental investigation of a dual purpose solar heating system. *Energy Conversion and Management*, Vol. 78, pp. 359-366. https://doi.org/10.1016/j.enconman.2013.10.046

Singh S., Dhiman P. (2016). Thermal performance of double pass packed bed solar air heaters – A comprehension review. *Renewable and Sustainable Energy Reviews*, Vol.53, pp. 1010-1031. https://doi.org/10.1016/j.rser.2015.09.058

Singh S., Kumar S. (2012). New approach for thermal testing of solar dryer: Development of generalized drying characteristic curve. *Solar Energy*, Vol. 86, pp. 1981-1991. https://doi.org/10.1016/j.solener.2012.04.001

Skaar C. (1988). Wood-water relations. Springer series in Wood Science. Springer Verlang, p. 278.

Souza G. F. M. V., Miranda R. F., Lobato F. S., Barrozo M. A. S. (2015). Simultaneous heat and mass transfer in a fixed bed dryer. *Applied Thermal Engineering*, Vol. 90, pp. 38-44. https://doi.org/10.1016/j.applthermaleng.2015.06.088

Tonui J. K., Tripanagnostopoulos Y. (2007). Improved PV/T solar collectors with heat extraction by forced or natural air circulation. *Renewable Energy*, Vol. 32, No.4, pp. 623-637. https://doi.org/10.1016/j.renene.2006.03.006

Torki-Harchegani M., Ghanbarian D., Pirbalouti A. G., Sadeghi M. (2016). Dehydration behaviour, mathematical modelling, Energy efficiency and essential oil yield of peppermint leaves undergoing microwave and hot air treatments. *Renewable and Sustainable Energy Reviews*, Vol. 58, pp. 407-418. https://doi.org/10.1016/j.rser.2015.12.078

Verma S. K., Prasad B. N. (2000). Investigation for the optimal thermohydraulic performance of artificially roughened solar air heaters. *Renewable Energy*, Vol. 20, No.1, pp. 19-36. https://doi.org/10.1016/S0960-1481(99)00081-6